View metadata, citation and similar papers at core.ac.uk
brought to you by CORE
provided by Archivio istituzionale della ricerca - Politecnico di Milano

UARC #1431727, VOL 00, ISS 00

Probabilistic life-cycle assessment and rehabilitation strategies for deteriorating structures: a case study

Elsa Garavaglia, Noemi Basso, and Luca Sgambi

QUERY SHEET

This page lists questions we have about your paper. The numbers displayed at left can be found in the text of the paper for reference. In addition, please review your paper as a whole for correctness.

Q1: Au: Please provide an abstract of up to 250 words for the article.
Q2: Au: Please provide missing corresponding author details.
Q3: Au: Please review all section headings in text to for accuracy.
Q4: Au: Please provide missing [Publisher location] for [Avramidou, 1990].
Q5: Au: Please provide missing [Publisher location] for [Baruchello and Assenza, 2004].
Q6: Au: Please provide missing [Publisher name] for [Binda et al., 2009].
Q7: Au: Please provide missing [Publisher location] for [Campanella, 2017].
Q8: Au: Please provide missing [Publisher location] for [Cigni, 1978].
Q9: Au: Please provide missing [Publisher location] for [Colombo, 1890].
Q10: Au: Please provide missing [Publisher location] for [Sandrinelli, 1905].

PROOF ONLY

TABLE OF CONTENTS LISTING

The table of contents for the journal will list your paper exactly as it appears below:

INTERNATIONAL JOURNAL OF ARCHITECTURAL HERITAGE
2018, VOL. 00, NO. 00, 1–16
https://doi.org/10.1080/15583058.2018.1431727

Taylor & Francis
Taylor & Francis Group

Check for updates

Probabilistic life-cycle assessment and rehabilitation strategies for deteriorating structures: a case study

Elsa Garavaglia[a], Noemi Basso[b], and Luca Sgambi[c]

[a]Department of Civil and Environmental Engineering, Politecnico di Milano, Milan, Italy; [b]School of Creative Science and Engineering, Department of Architecture, Waseda University, Tokyo, Japan; [c]Faculty of Architecture, Architectural Engineering and Urban Planning, Université catholique de Louvain, Louvain-la-Neuve, Belgium

KEYWORDS life-cycle; Monte Carlo simulation; structural aging

PROOF ONLY

1. Introduction

Interdisciplinary expert interaction is always complicated but crucial in building restoration, even more when the structure is protected by cultural heritage regulations. Respecting the structural, architectural, and historic qualities of the building, experts must cooperate together in order to define the optimal intervention solution.

When it comes to rehabilitation, a good knowledge of building regulations development and a thorough analysis are the key to success. The analysis process should be based on historic, formal, and structural investigations in order to identify the main phases of the building from design concept, through service life, until current conditions. Then, accurate inspections and material survey are the correct way for diagnosis of a structure defect and successive intervention plan (Binda et al. 1996a; Binda 1996; Mahin, 1998, Cardani et al. 2001; Lourenço, Luso, and Almeida 2006; Campanella 2017). Whenever there is evidence of a significant deterioration, it is fundamental to focus on quantifying the structural residual bearing capacity. This is of particular importance when restoring and converting existing buildings (Avramidou, 1990; Baruchello and Assenza 2004; Binda et al. 1999, 1996b; Campanella 2017; Cigni 1978; de Vent et al. 2010; Lagomarsino and Cattari 2015; Lourenço 2006; Lourenço et al. 2013).

Structural diagnostics provides a comprehensive analysis of damage patterns in structural systems, especially when surveys are detailed and accurate (Avramidou, 1990; Baruchello and Assenza 2004; Binda et al. 2009, 2011, 2005; Yang et al. 2004; Yoa, Chang, and Lee 1992).

Non-destructive (e.g., crack monitoring, sclerometer tests, infrared thermography, ground-penetrating radar, sonic/ultrasonic tests, etc.) and minimally invasive (e.g., flat-jack tests, pull-out tests, drilling techniques, etc.) diagnostic techniques play a relevant role in studying the conditions of existing construction without causing excessive disturbance or disruption to the building fabric (Bagnoli et al. 2015; Bertolini et al. 2004; Binda et al. 2011; Gregorczyk and Lourenço 2000; Hobbs and Tchoketch Kebir 2007; Lo and Choi 2004; Schuller 2003). However, these techniques are often applied locally in order to cause minimal damage (i.e., partially invasive and destructive tests) and minimize operating costs.

Complex numerical simulations, based on data from structural diagnostics, are usually used to investigate the global structural response of existing systems (Koçak and Köksal 2010; Lourenço and Rots 1997; Lourenço, Rots, and Blaauwendraad 1998; Melchers and Frangopol 2008; Roca et al. 2010). Several uncertainties are involved in model processing. This is true particularly for deteriorated structures. Results from numerical simulations are approximations of the real structural behavior. However, when the model is adequately calibrated with credible data, the quantitative output, though representing only one aspect of the problem, is a good support for highlighting the structural vulnerabilities where investigations should be focused on and optimize the diagnostic process (Sousa, Branco, and Lourenço 2014).

As a matter of complexity, the investigation of structural life cycle needs to adopt a rigorous hierarchical procedure as follows: (1) identifying the key points of the problem; (2) considering each point separately; (3) evaluating possible synergistic interactions between key points; and (4) global simulation. This process has been the basis for the development of advanced decomposition techniques and intervention strategies (Biondini, Bontempi, and Malerba 2004; Bontempi, Catallo, and Sgambi 2004; Decò and Frangopol 2013; Furuta et al. 2008; Petrini and Bontempi 2011).

However, because of the high uncertainty affecting the problem, this approach cannot be applied to old masonry buildings, where the simulation of wall response particularly around wall-to-wall and wall-to-beam joints lacks in

CONTACT Elsa Garavaglia elsa.garavaglia@polimi.it
© 2018 Taylor & Francis

reliability. Interesting studies on this topic have been done so far and the research developments seem promising (Bruggi 2014; Milani and Lourenço 2010; Roca et al. 2010).

Modeling the damage evolution of a structural element during its service life can be very useful in supporting diagnostic campaign and the formulation of intervention strategies when parts of the system are too small to be investigated or too difficult to be reached (Cruz et al. 2015).

This research aims to demonstrate the validity of a probabilistic approach to life cycle management of existing structures, which investigates the deterioration process affecting a system, identifies which element is most likely to fail, and supports risk-aware rehabilitation and strengthening strategies.

An adaptable deterioration law implemented in a structural analysis code has been applied to simulate the damage evolution over the service life of complex systems. The deterioration law models the uncertainties involved in damage and aging processes over time. The selection of a proper probability density function that reflects the fluctuation of parameter values along with a Monte Carlo simulation can provide a fairly reliable estimation of damage magnitude over time.

Then, thanks to the sampling generated with Monte Carlo method, several maintenance scenarios related to risk level, time, and costs can be determined and analyzed.

The procedure here described is based on studies of ideal examples (Garavaglia, Basso, and Sgambi 2012) and new constructions (Garavaglia and Sgambi 2016). In this article, the methodology has been applied to a historically significant case study, characterized by two distinct phases in its life cycle: operation (deterioration by natural aging and usage) and obsolescence (degradation by negligence and weathering). These stages have required the application of two different deterioration laws.

This study analyzes the steel frame roof structure of the old pig abattoir within the complex of the municipal slaughterhouse in Monza (close to Milan, Northern Italy). The construction was built in 1902, and abandoned in 1984. The second phase of life, still ongoing, has significantly sped up the degradation process.

The primary structure, composed by a roof steel truss system, has survived both the abandonment and the negligence, while the secondary structure, characterized by timber purlins, rafters, and roof battens, and terracotta tiles, has almost entirely been lost.

The Cultural Heritage Authority requires at least the protection and preservation of the primary structure. Therefore, at first, it is fundamental to evaluate the steel truss residual bearing capacity under design static loading and investigate the possible maintenance actions.

Section 2 follows chronologically the main events characterizing the slaughterhouse life, from design to disuse, and briefly describes the structure of the pig abattoir building. Section 3 summarizes the main points of the Monte Carlo simulation applied to the roof truss case study. Structural geometry, loads, structural model, and damage constitutive laws referred to pre-disuse and post-disuse are described in detail in Section 4, as are the simulation results. Section 5 discusses the probabilistic evaluation of failure times. Then, Section 6 investigates the possible interventions scenarios in terms of costs, and after-maintenance reliability and safety.

2. Case study: the old pig abattoir in Monza

2.1 Chronology of the construction phases

At the end of the 19th century (1889–1890), a national law made it mandatory for municipalities bigger than 6,000 people to confined animal slaughtering in prescribed places, called "Macelli" (i.e. abattoirs). The first attempt for the design of the municipal slaughterhouse in Monza was made by engineer Arpesani in 1894 (Monza, file 629/1, June 6, 1894). Both the design report and the application for building permit are still available for consultation. Arpesani's proposal consisted in a 4950 m^2 complex with a sewer system controlling the wastewater disposal. The distribution and spatial organization optimized functions and management. The project included also an administration plan divided in two phases: a 50-year term managed by the building contractor company, followed by the transfer of the whole complex under Monza Municipality's authority. Nevertheless, there is no evidence of this agreement.

Engineers Pinciroli and Riboni presented a new proposal, with a different location, in 1896. That time the project met the required criteria of the Provincial Administration (April 6, 1901). The same year, the project was finalized by Municipal engineering and design department under the direction of engineer Jotta. As per Pinciroli and Riboni's concept, the 3500 m^2 construction site was located in a strategic position, along an important directional axis, close to Villoresi Canal (ship canal). The distribution and functional organization were well conceived too: waiting buildings ran along E-W axis for shading optimization; meat-processing buildings ran along N-S axis for lighting optimization (Figure 1).

Although the pig abattoir was built between 1901 and 1902, the construction works for the whole complex of the slaughterhouse lasted five years and ended with the official opening ceremony in 1907 (Monza, file 630/1, August 9, 1902).

Some questionable and architecturally incoherent changes were made while the complex was under

PROOF ONLY

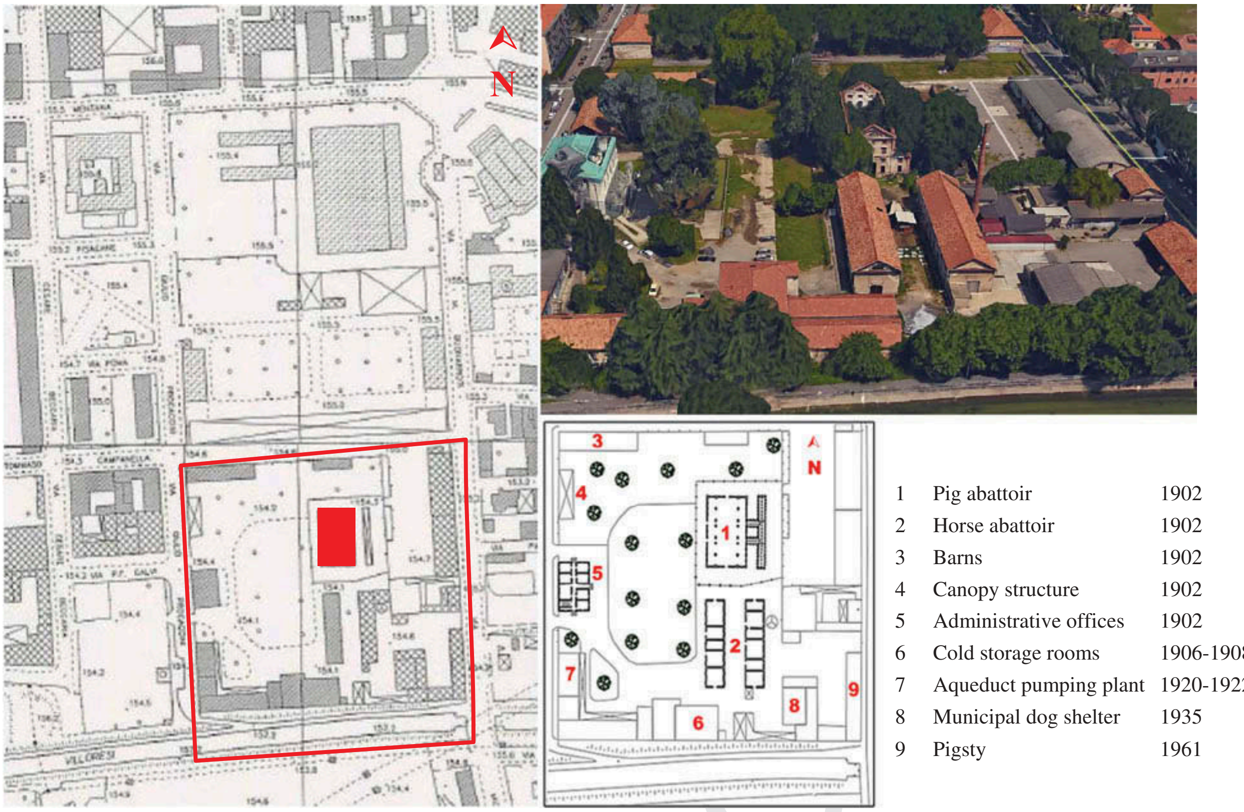

a) b)

Figure 1. (a) Photogrammetric analysis of municipal slaughterhouse area. The pig abattoir is highlighted in red; and (b) slaughterhouse complex plan (Cartographic material from Municipal Archive of Monza, 2004).

construction. In 1906, a new law about meat preservation and storage made it necessary the hasty addiction of cold storage rooms. This intervention was completed in 1908. At the beginning of the 1920s the slaughterhouse area was affected by urban infrastructure implementations (i.e., municipal aqueduct) and functional facilities reorganization and integration (i.e., contaminated meat storage areas and pig gallery respectively). Works finished in 1922.

In the 1960s, the pigsty was turned into an administrative office of the near livestock market (built in 1913). The S-E waiting area became a warehouse of a road maintenance company. In 1984, the whole complex was definitely shut down. The great snow of 1985 that blanketed Lombardy caused the collapse of the entire cattle area and the partial failure of the pig area.

Public Administration asked for the demolition of the slaughterhouse complex, but the Cultural Heritage Authority stood up against the request with an act protecting the whole area (May 8, 1985).

2.2 Pig slaughterhouse structure

The pig slaughterhouse building (1902) is isolated on all sides, but the East façade where two limbs of a canopy structures are built up against the perimetral wall (Figure 1b, building n. 1).

The structure has a rectangular plan measuring 32.00 m North–South by 18.26 m East–West (inner space). There are no middle floors. The architectural typology clearly refers to industrial structures, with a bridge crane on rails by means the carcasses were moved. Although heavily damaged, the crane-rails system still remains standing. Thanks to a scrupulous use of aesthetics and construction design and techniques, this building can be considered a good example of great value in industrial architecture. The basilica-like plan is divided into 3 aisles: the nave is 32.00 m long, 10.00 m wide, and 14.60 m high; the side-aisles are 3.50 m wide and 8.40 m high (Figure 2).

At the top of the central aisle wall there are 12 1 × 1.40 m glassless windows, with a shading system for ventilation and steam discharge. Above these windows there are five arches with a 5.00 m span and a 7.00 m height, and two arches with a 2.50 m span and a 6.00 m height at the side doors. On the side-aisles there is a double series of 12 windows: the upper ones measure 1 × 1.40 m and are glassless with shading screens, while the lower ones are common windows of 1 × 2.30 m. An entrance is located on each side of the building. The main

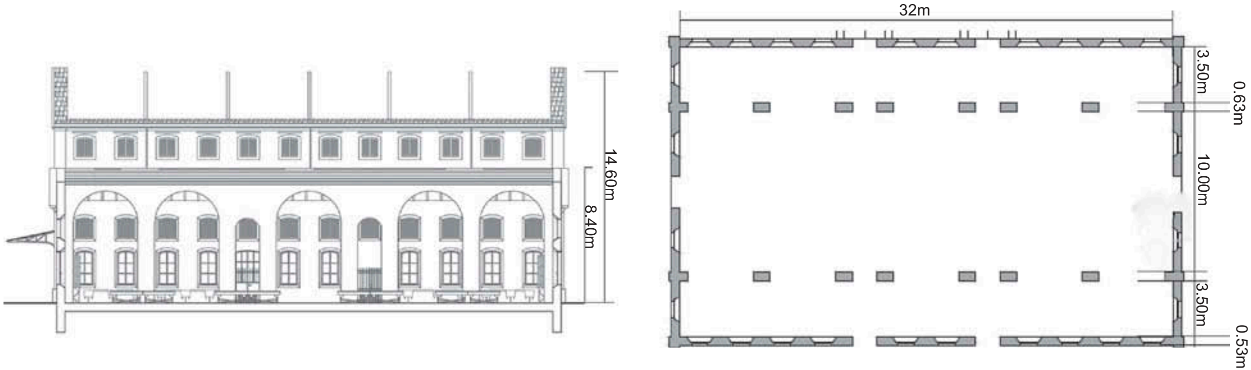

Figure 2. Pig abattoir: plan and elevation (scale 1:500).

accesses are both on the North side, with a steel frame door, and on the South side, with a simple gate. A simple gate and a gate plus a steel frame door with glass respectively close the secondary entrances on East and West sides.

The whole building is a 53 cm-thick (i.e., lateral walls) and 63 cm-thick (i.e., spine walls) masonry structure. Based on historic evidences about construction and design techniques, the wall stratigraphy is most likely to consist of solid masonry. Because this assumption significantly affects the structural analysis, any reinforcement strategy considered should rely on a careful investigation of the wall construction typology. The loss of plaster at the top has exposed the wall-to-wall joints, revealing a well-conceived, still efficient anchorage. Depending on the location, the roof structure presents two different typologies:

- lateral aisles: timber roof truss with longerons, purlins, rafters, and roof battens; and
- nave: 5-steel-truss system (i.e. Polonceau truss) fixed to the walls, with a secondary timber structure (i.e., purlins, rafters, and roof battens) and a tile roof covering (Figure 3).

2.3 Disuse and abandonment

According to official documentation, the pig abattoir seems not to have been affected by any of the integrations or functional transformations done to the slaughterhouse complex, and preserved the original function until the shutdown in 1984.

Since the disuse, the exceptional snowfall in 1985 has caused a partial collapse of the roof covering, exposing the above steel truss structure to weathering. From 1984–2015 (i.e., most recent in-situ surveying) the degradation process got worse and worse due to negligence.

The 2005 survey reported damage to the timber roof system and widespread loss of plaster caused mostly by the inefficiency of the eaves. The nave roof steel-truss system showed 1st-stage corrosion evidences due to aggressive environment.

PROOF ONLY

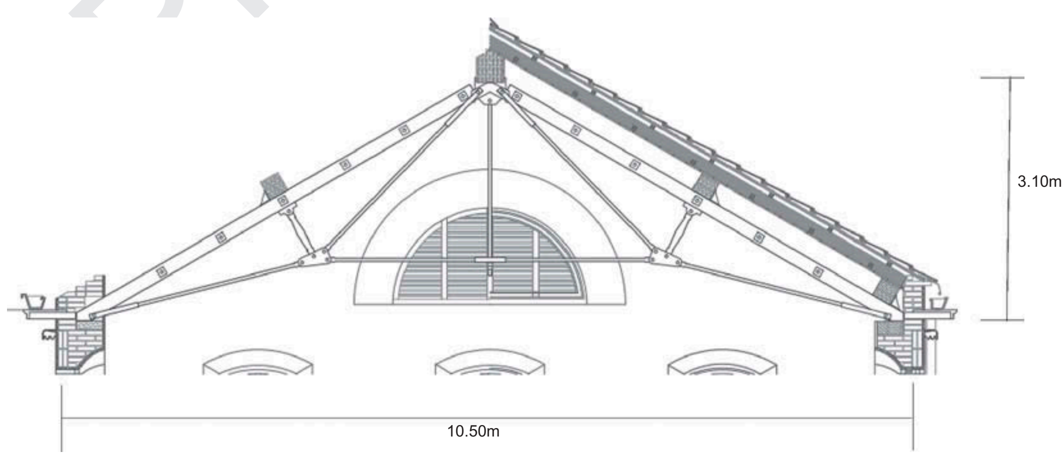

Figure 3. Nave roof system, original layout. The steel truss structure (primary system) is shown in white, while the original timber structure (secondary system) is highlighted in grey.

Figure 4. Pig slaughterhouse at present time.

In 2015, the roof covering was almost completely collapsed, the corrosion spread out, and tie-rods were affected by mild steel relaxation. Furthermore, timber elements appeared to be wholly degraded, and the masonry structure presented significant instability problems mainly due to wild vegetation (Figure 4).

Because the pig abattoir is protected by law, it cannot be demolished but preserved, therefore any intervention to re-use or change the use requires previous structural strengthen works to secure the building and the conservation of its significant or most character-defining elements. The nave roof system represents a distinctive element of the structure.

The analysis of the deterioration process affecting the steel truss over the building service life is presented here. It includes a residual load-bearing capacity estimation, and a cost-performance comparison between different maintenance strategies considering two intervention scenarios (i.e., right after the disuse, and at present conditions).

3. Monte Carlo simulation: approach explanation

The proposed approach aims to investigate the roof-system life cycle, identifying the main structural vulnerabilities, estimating its residue resistance, and planning possible retrofit strategies while preserving its structural and historic identity. Visual inspection and diagnostic campaign are of extreme importance in defining the current state of the system. However, the slenderness of the steel roof truss and the high risk of compromising the structure using invasive tests are the main reasons for proposing a numerical probabilistic analysis based on limited data and without further monitoring support.

The lack of information about the deterioration process affecting the structural elements is bypassed using a Monte Carlo simulation implemented with a damage law. This integrated method enables to investigate different environmental conditions affecting the structure during its life (Biondini, Frangopol, and Garavaglia 2008; Garavaglia, Basso, and Sgambi 2012; Garavaglia and Sgambi 2016). Garavaglia and Sgambi developed the methodology in a previous work (Garavaglia and Sgambi 2016) where it was used to study the service life of a new steel bridge. In this article, the procedure has been expanded to evaluate the life cycle of a deteriorated roof system, considering two main stages in its life (more details in Garavaglia and Sgambi 2016). While in Garavaglia and Sgambi (2016) the methodology was applied to investigate the service life of a newly designed steel bridge, this article focuses on the analysis of a steel roof truss affected by severe, diffuse deterioration. The two studies show differences in parameters' choice and calibration.

A newly designed structure provides a higher confidence level for mechanical properties of materials, and general mechanical response of the whole system. Furthermore, the construction site is safe and the structural details can be verified directly in situ.

On the contrary, the intervention on existing, old structures is more complicated due to lack in design data (when design reports were missed or destroyed), inaccessibility for direct observation (i.e., dangerous, unsafe buildings), lack of historic data concerning loading and extraordinary event occurrences, insufficient financial funds for field and diagnostic surveys. These difficulties significantly increase the uncertainty affecting the analysis, and require a probabilistic approach. However, a careful calibration of both structural model and parameters is essential for guaranteeing the efficiency of the method. Therefore, field and diagnostic surveys, and historic formal and structural investigations, are fundamental components of the whole methodology.

The analysis of a new structure aims to define possible maintenance strategies to be applied when needed. But the investigation of an old structure is usually used to point out administrative misbehaviors (i.e., lack of ordinary maintenance), and need for urgent interventions in order to avoid the worsening of damage and deterioration processes, or even worse the irreparable loss of cultural heritage.

PROOF ONLY

3.1 Key methodological points

- The Monte Carlo based method estimates the structural reliability of the system subjected to a simulated compound deterioration, knowing its geometric and mechanical conditions.
- Thanks to the probabilistic variation of the parameters involved in, the implementation of a damage law together with the Monte Carlo code, allows the simulation of possible damage associated with loading and weathering. The deterioration law is chosen according to real data collected through surveys. The probabilistic distribution used to assess the parameters is decided considering physic assumptions concerning the damage process.
- The structural analysis is applied to a 1,000-sample dataset. A sample size of 1,000 provides an adequate and reliable level of confidence with a CV of probability of failure upper threshold of 0.2, without wasting a large amount of time.
- The method investigates the structural response of each sample, instant-by-instant up to failure time, in terms of material strength σ.

3.2 Damage law

Assuming the deterioration law to be adequately adaptive, the calibration of initial parameters to be credible, and the probability distribution related to parametric variation to be effective, a Monte Carlo simulation employing a large data sampling results in predicting the damage evolution of a structure when few experimental data are available (Garavaglia and Sgambi 2015).

In the case study discussed here, the degradation law employs a damage index δ to probabilistically describe the percentage loss of structural capacity affecting each element over time. In particular, physical observations have addressed the cross-section decrease as the major damage. The sectional area decreases along with the load-bearing capacity and the material ultimate stress $\bar{\sigma}$. When it comes to very slender elements it might be the main reason of sudden collapse.

With regard to the above-mentioned considerations, the damage index can be described as:

$$A(t) = A_0[1 - \delta(t)] \tag{1}$$

$$\bar{\sigma}(t) = \bar{\sigma}_0[1 - \delta(t)], \tag{2}$$

where subscript *0* refers to parameters in non-damaged conditions.

The damage index $\delta = \delta(t) \in [0;1]$ describes the time-dependent deterioration process as:

$$\delta(t) = \begin{cases} \omega^{1-\rho}\tau^{\rho}, \ \tau \le \omega \\ 1-(1-\omega)^{1-\rho}(1-\tau)^{\rho}, \ \omega < \tau < 1 \\ 1, \ \tau \ge 1 \end{cases}, \tag{3}$$

where $\tau = t/T_1$, T_1 is the *n*-instant of failure related to the damage threshold $\delta = 1$; ρ and ω are shape parameters defining the deterioration process due to the combination of loading and weathering:

$$\rho = \rho_a + (\rho_b - \rho_a)\xi \tag{4}$$

$$\omega = \omega_a + (\omega_b - \omega_a)\xi, \tag{5}$$

where the coefficient $\xi = \sigma/\bar{\sigma}$ describes the ratio between the stress level σ at *n*-instant and the design limit state for a generic structural element. The subscript *a* refers to damage associated with weathering, while the subscript *b* refers to damage associated with loading.

Changes in ρ and ω significantly affect the law (3) (Figure 5). When the calibration of the initial parameters is supported by accurate experimental data, and the optimal probability distribution reflecting the time-dependent variation of data is chosen, the law (3) can describe the damage evolution associated with aggressive environment and natural aging.

In the case study proposed here, the damage is considered in terms of cross sectional area reduction as shown in Equation (1).

3.3 Monte Carlo simulation

In order to investigate the life-cycle of the structure over time, along with the damage affecting it, a Monte Carlo simulation implemented with the deterioration law (3) is run. Shape parameters ρ_a, ρ_b, ω_a, ω_b, and failure time T_f are modeled as random variables with assigned probability distributions. The probability distributions are chosen according to physic phenomenon properties and behavior in the tails where rare events are more likely to occur (Garavaglia, Gianni, and Molina 2004).

In the case study area, aggressions by weather follow an annual cyclical pattern, except for extraordinary events as the exceptional snowfall in 1985. Because the damage observed is almost the same on each structural element of the roof system, the shape parameters ρ and ω in the degradation law have been modeled with a Normal distribution, in accordance with several examples in scientific publications (Ceravolo, De Stefano, and Pescatore 2009; Ciampoli 1998, 1999). Then, assuming the failure

PROOF ONLY

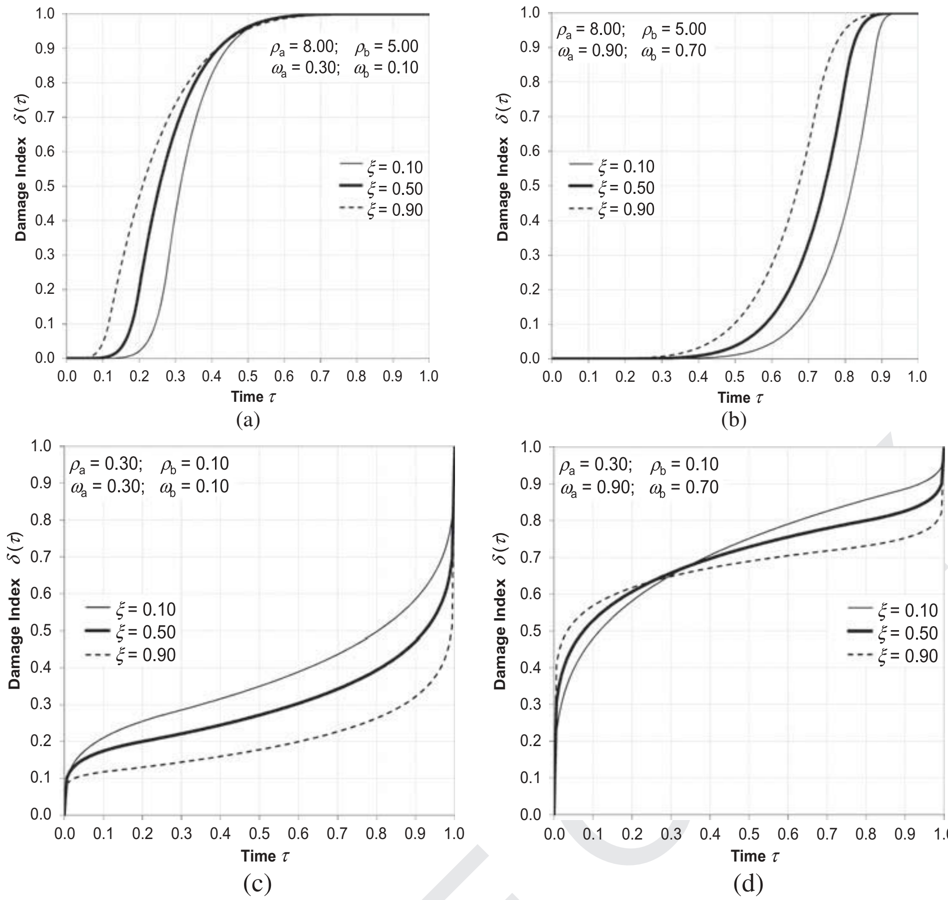

Figure 5. Material damage index δ vs time $\tau = t/T_f$. Damage law for different level ξ of performance loss, and different values of parameters ξ e ω.

probability and the sudden collapse probability of a deteriorated system to be time dependent, the failure time T_f has been modeled using a Gamma distribution (Table 1). The hazard rate of Gamma distribution asymptotically increases over time and it well represents the risk of immediate occurrence of a sudden collapse in the case study structure (Garavaglia, Gianni, and Molina 2004).

Therefore, based on mean and standard deviation processed from data collected, the numerical code can compute the probability distributions (Table 1). Using the *rand* function of MatLab (The Matworths Inc. 2005), the code makes a random choice of values from the probability distributions computed. Then the random numbers are implemented to generate 1,000 damage laws. Each damage law results in 1,000 structural responses. That means: a random value from the assigned probability function is given to the variables each run, and implemented in the law (3). Then the deterioration law is applied to the time-dependent structural analysis and it provides the structural response in terms of loss of stiffness member by member and failure time for the entire structure.

Significant data can be obtained with this procedure: a variety of failure time samples for mean failure time $\bar{T}_{fail}$ assessment and related probability density function $F_{fail}\ (t)$ estimation, and the variation affecting geometries and mechanical properties of each structural element (more details in Garavaglia and Sgambi 2016).

Table 1. Monte Carlo simulation: input parameters and related standard deviation. Random variables with mean value, variation, and distribution are listed.

	First phase 1902–1985			Second phase 1985–2015		
Damage law parameters	Mean value	Standard deviation	Distribution	Mean value	Standard deviation	Distribution
ξ_a	5.50	0.2	normal	6.00	0.2	normal
ξ_b	3.50	0.2	normal	3.00	0.2	normal
ω_a	0.95	0.02	normal	1.00	0.02	normal
ω_b	0.75	0.02	normal	0.30	0.02	normal
T_{fail} (yrs)	130	15	gamma	70	30	gamma

Figure 6. Roof truss system details (Dall'Orto, Sanchez, Suma, 2015).

4. Nave roof truss system

Figure 6 shows the roof truss system covering the central nave of the pig abattoir.

The central aisle is covered with a 5-steel-truss system with a secondary timber structure and a tile roof covering. Since the shut down in 1984, the great snowfall of 1985 caused the roof covering to partially collapse, and the steel trusses to be exposed to environmental aggression.

The life-cycle investigation here presented considers the case study life span from construction to present time, dividing it in pre-disuse (i.e., service life) and post-disuse (i.e., obsolescence). During this time, the roof structural system has been damaged by: natural aging and usage (mainly pre-disuse phase), and negligence and weathering (post-disuse phase). These different causes require the application of two different deterioration laws.

Therefore, the method explained in Section 2 must be applied twice with a different calibration of damage parameters in law (3), in order to analyze the structural life cycle during service life and then, starting from the damage conditions achieved at the time of disuse, evaluate the response under environmental degradation. The parameter calibration was executed using historic information and data collected during surveys in 1985, 2005, and 2015.

Cross-section decrease (percentage) collected from direct and photographic observations and was used for the parameter calibration. The first damage law was calibrated according to the data collected right after the collapse of the roof; the second law calibration is based on the data collected during the surveys in 2005 and 2015. The parameters are obtained by identification, where the consequent damage law must agree with the deterioration value observed during the surveys: 1985, cross-section loss equal to 10–30%, 2005 increase in cross-section loss equal to 3–5%, 2015 additional cross-section loss of 7–10% (see Table 1 and Sections 3.2 and 3.4). The identification process provides a mean value for each parameter's behavior; the standard deviation was chosen in accordance with examples in publications on similar topics (Ceravolo, De Stefano, and Pescatore 2009; Ciampoli 1999).

4.1 Roof structural system geometry

The case study structure is a Polonceau truss composed by small tension and compression iron bars (Table 2).

The original load on the structure was estimated to be approximately 2.7 kN/m^2 on an influence area of 57.5 m^2. Figure 7 shows the truss geometry and the forces applied at each node. The Monte Carlo simulation refers to the static model in Figure 7b.

4.2 Aging process

According to historic evidences about construction and design techniques applied to the case study (Cartographic material from Municipal Archive of Monza; degree theses by Dall'Orto et al., 2015; Porro and Vezzani 2005), and considering the historic building code adopted (Colombo 1890; Sandrinelli 1905) the ultimate stress $\bar{\sigma}_{ultimate}$ equal to 3087 kg/cm^2 (i.e., 308.7 MPa) has been assumed as reference value. The diagnostic campaign performed after the partial collapse of the roofing in 1985 has highlighted a limited deterioration level of the roof structure. The mean damage detected is likely to be between 10% and 30% in 83 years of life. Both environmental and mechanical factors have been considered as the main causes of deterioration. The parameters in the damage law (3) were evaluated considering a service life lower threshold T_f equal to 130 years and a simulated damage level after 83 years from the construction close to the one observed. That resulted in a $\tau \cong 0.6$, and a damage index δ between 0.1 and 0.3, depending on ξ. The parameters ρ_a, ω_a and ρ_b, ω_b were determined by a simple least square

Table 2. Original geometry and mechanical properties of steel truss elements.

Members	Cross section	L cm	A_0 cm^2	V_0 cm^3	I_0 cm^4
1–4	I	304.60	32.00	9747.20	682.67
5, 8	O	318.00	13.00	4134.00	13.44
6, 7	O	215.00	13.00	2795.00	13.44
10, 12	O	322.00	13.00	4186.00	13.44
11	O	240.00	13.00	3120.00	13.44
9, 13	O	97.36	17.00	1655.12	23.55

PROOF ONLY

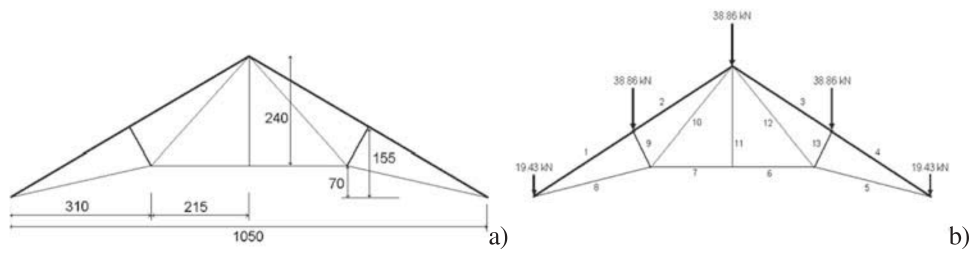

Figure 7. (a) Truss geometry (uom: cm); and (b) truss static model.

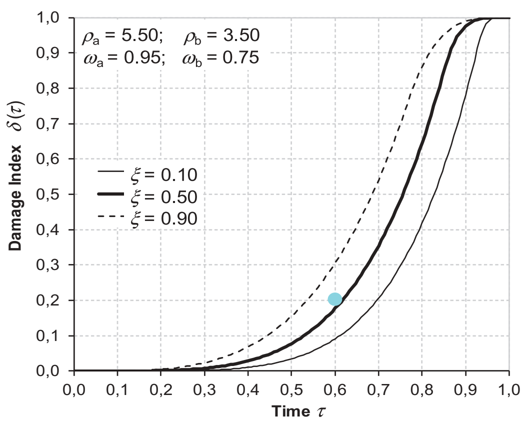

Figure 8. Damage index δ vs. normalized time $\tau = t/T_f$ referred to percent loss of performance ξ (first hypothesis). Light blue dot shows the damage level post-disuse (1985 survey).

method. Figure 8 shows the mean values of the initial damage parameters with standard deviations of 0.2 for ρ and 0.02 for ω, and the deterioration law obtained. T_f was assumed to be equal to 132 years with a standard deviation of 15 years.

4.3 Monte Carlo simulation: use stage

When the deterioration law is defined, the Monte Carlo program can simulate the damage affecting each truss element.

Table 2 shows the system geometry. At first the system is assumed to be undamaged with a homogeneously distributed deterioration except for elements 1–4 subjected to a heavier deterioration in the lower part due to usage. The structural analysis, implemented with the law (3) and applied to 1,000 samples, describes the deterioration process in terms of cross-section decrease, load-bearing capacity decrease (i.e., material strength σ), maximum strain, and time-instant $\hat{t}$.

After 83 years exposed to damage law (3), the roof system presents a simulated cross-section decrease of about 27% (Table 3).

Data recorded in 1985 (Documents from Municipal Archive of Monza) seem to validate the simulation

Table 3. Geometry and mechanical properties of truss elements post-disuse (1985). The figure below the table shows the loss of volume related to the loss of cross-section area.

Members	Cross section	Loss of A_0 (%)	A_1 cm^2	Loss of V_0 (%)	V_1 cm^3	I_1 cm^4
1–4	I	27.2	23.94	27.2	7095.51	382.20
5, 8	O	27.4	9.61	27.4	3000.88	7.70
6, 7	O	27.4	9.61	27.4	2028.90	7.70
10, 12	O	27.4	9.61	27.4	3038.63	7.70
11	O	27.4	9.61	27.4	2264.82	7.70
9, 13	O	26.7	12.32	26.7	1213.49	12.65

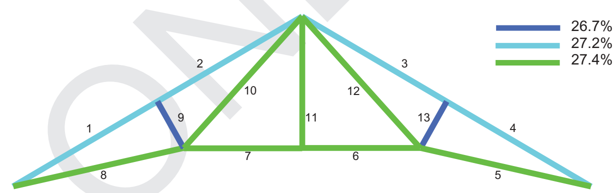

results: at that time, the damage was estimated to be in the range from 10–30% on all the observable structural members.

The structural analysis of the post-disuse period (from 1985–2015) started from the results obtained with the first run of Monte Carlo simulation.

4.4 Weathering and negligence

Since the disuse, although the structural elements have been affected by significant corrosion, the roof system still preserves a residual bearing capacity. In order to evaluate the opportunity to restore and reuse the structure, the truss system response after the collapse of the roof must be simulated. At this time, the structure is assumed affected by its own weight and weathering.

The post-disuse analysis and modeling required a new deterioration law. According to data by Porro e Vezzani (2005), damage got an increase close to 5% right after the disuse, while 2015 surveys (Dall'Orto et al. 2015) recorded a 10% increment of cross-section loss in most of the structural members (i.e., 40% damage). Thence, considering these observations, new damage parameters were defined (Figure 9).

PROOF ONLY

Table 4. Geometry and mechanical properties of truss elements at 2015. The figure below the table shows the loss of volume.

Members	Cross section	Loss of A_0 (%)	A_2 cm^2	Loss of V_0 (%)	V_2 cm^3	I_2 cm^4
1–4	I	34.15	21.07	34.15	6418.10	295.98
5, 8	O	34.45	5.68	34.45	1806.63	2.69
6, 7	O	35.17	8.43	35.17	1811.91	5.92
10, 12	O	34.39	8.53	34.39	2746.47	6.06
11	O	34.61	8.50	34.61	2040.29	6.02
9, 13	O	31.79	11.60	31.79	1128.99	11

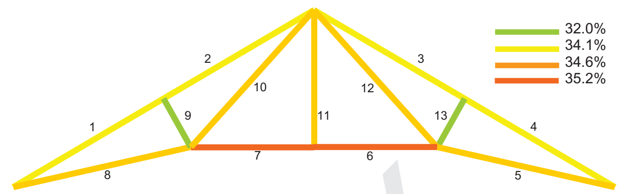

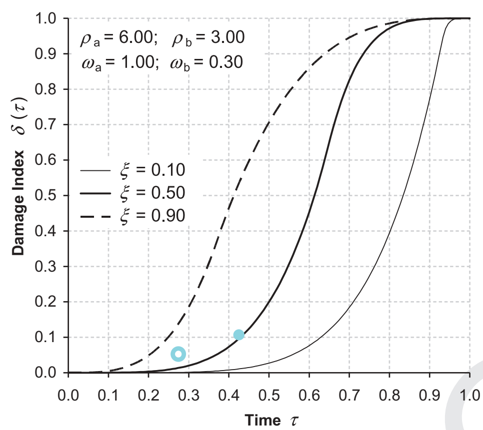

Figure 9. Damage index δ vs. normalized time $\tau = t/T_f$ related to percent loss of performance ξ (second hypothesis). Light blue ring shows the damage level at 2005; light blue dot shows the damage level at 2015.

Degradation depends on both environmental and mechanical factors. For the damage parameter assessment, it was assumed a failure time T_f with lower threshold of 70 years, and a simulated damage level 20 years and 30 years after the disuse close to the one observed. That implied a damage index δ between 0.05 and 0.1 for $\tau \cong 0.28$, and a damage index δ between 0.1 and 0.4 for $\tau \cong 0.43$, depending on ξ. The parameters ρ_a, ω_a and ρ_b, ω_b were determined again by a simple least square method. Figure 9 shows the mean values of the initial damage parameters with standard deviations of 0.2 for ρ and 0.02 for ω, and the deterioration law obtained. T_f was assumed to be equal to 70 years with a standard deviation of 30 years.

4.5 Monte Carlo simulation: post-disuse stage

When the new damage law describing the deterioration process post-disuse (till the most recent survey in 2015) is defined, it's time to run the Monte Carlo simulation again. Table 2 shows the truss geometry resulted from the first simulation. At this time the system is assumed already damaged with a homogeneously distributed deterioration, and affected by its own weight due to the almost total collapse of the roofing. The structural analysis, implemented with the law (3) along with the new parameters is applied to 1,000 samples, and it describes the deterioration process in terms of cross-section decrease, load-bearing capacity decrease σ, maximum strain, and time-instant $\hat{t}$.

Table 4 shows the results of this second simulation. 30 years after the roofing collapsed, the modeled system exposed to deterioration law (3), presents a significant increase of damage level due to weathering and negligence.

5. Failure time assessment

The structural analysis is performed on all the samples generated. For each iteration the interval to the failure time T_{fail} is registered. A failure is assumed to occurr when the ultimate stress $\bar{\sigma}_{ultimate}$ or the ultimate strain of one of the nodes in one of the plane directions $u_{\max}$ and $v_{\max}$ are exceeded (Garavaglia and Sgambi 2016). A sample size of 1,000 is larger enough to ensure that the results obtained from the Monte Carlo simulation are consistent with the real structural behavior over time, even though in probabilistic terms. Any intervention scenario (repairs and future maintenance plans) resulting from the evaluation of the simulation outcomes can be disregarded by sudden and unexpected events, which may threaten the structure when it is at its highest level of vulnerability (i.e., instant right before the maintenance time). However, the uncertainty related to

PROOF ONLY

unpredictable occurrences is unavoidable but the consequent level of risk is acceptable.

5.1 Probability distribution function of the failure time t_{fail}

The failure time T_{fail} obtained from the 1,000 simulations was modeled with a Gamma distribution $F_{fail}\ (t)$. The choice of Gamma function for describing the distribution of failure time has been discussed in Section 2.3 (more details in Garavaglia, Gianni, and Molina 2004).

When the failure time distribution is defined, the probability of collapsing at a given state Δt after t_0 depends on the boundary condition the collapse never happened before t_0 and it is obtained by the following conditional probability of failure:

$$P_{\Delta t|t_0} = \frac{\left[F_{fail}(t_0 + \Delta t) - F_{fail}(t_0)\right]}{\left[1 - F_{fail}(t_0)\right]} \qquad (6)$$

estimated for a given interval Δt from the time already passed t_0 (i.e., t_0 = 82 years, case study service time 1902–1984).

The conditional probability (6) applied to the simulation discussed in Section 3.3 shows a structural failure risk level at 1985 (i.e., one year after disuse) still low, $P_{\Delta t=1|t_0=1984}$=0.0018. This result is validated by evidence: the structural system survived the collapse of the roof. However, considering present conditions, the conditional probability of failure $P_{\Delta t|t_0}$ is very high (Equation (6)). The risk affected the steel structure at 2017 (i.e., two years after the last analysis) is $P_{\Delta t=2|t_0=2015}$=0.128, that means more than twice the risk recorded in 1985.

Because the case study is protected by Cultural Heritage Authority, it is essential to prove the efficacy of prevention and maintenance strategy simulations in both structural reliability and people safekeeping. The procedure here discussed proves to be useful in defining effective intervention strategies.

6. Decision-making strategies: repairing vs. replacing

In terms of intervention strategies to be adopted on historic buildings, decision-making process is never as simple as it seems. This section discussed protection and maintenance scenarios in terms of short- and long-term cost-performance impacts.

The possible intervention scenarios are:

- *1985 repair*: repair of the whole roof structural system after the collapse in 1985;
- *2015 repair*: repair of the whole roof structural system in 2015;
- *2015 replace*: replacement of the whole roof structural system in 2015.

These scenarios have been compared in terms of cost using the method proposed by Kong and Frangopol (2003).

6.1 Cost investigation

Whenever maintenance solutions are investigated, actual cost of repair, construction site costs, costs directly related to the duration of the maintenance and to inconveniences caused by possible temporary unavailability of construction must be considered. Since the case study is under the authority of Cultural Heritage Institution, the analysis also includes costs related to the intervention techniques, which have to preserve its historic and architectural identity.

The life-cycle cost C_T over the expected lifetime T is the sum of the initial cost C_0 and the maintenance cost C_m (Flanagan, Norman, and Robinson 1989):

$$C_T = C_0 + C_m. \qquad (7)$$

The initial cost can sometimes represents the material volume cost:

$$C_0 = \sum_k c_{0k} V_k, \qquad (8)$$

where c_{0k} and V_k are the volume unit cost and the material volume of member k, respectively.

Considering a prescribed maintenance scenario, the total cost of maintenance C_m is known as the sum of the cost C_q of individual interventions (Kong and Frangopol 2003):

$$C_m = \sum_q \frac{C_q}{(1+\nu)^{t_q}}, \qquad (9)$$

where the cost C_q of the qth rehabilitation is referred to the initial construction time using a proper discount rate of money ν. The cost C_q of the individual intervention is assumed as Biondini, Frangopol, and Garavaglia (2008):

$$C_q = C_{\alpha q} + \sum_k \delta_{kq}(\chi\ c_{kq}) V_k, \qquad (10)$$

where $C_{\alpha q} = \alpha_q C_0$ is a fixed cost estimated as α_q percent of the initial cost C_0, δ_{kq} is the damage index of k-member, and c_{kq} is the volume unit cost for restoring the k-member. Then, in regard to the expected structural lifetime T, the annual cost C can be computed as Flanagan, Norman, and Robinson (1989):

PROOF ONLY

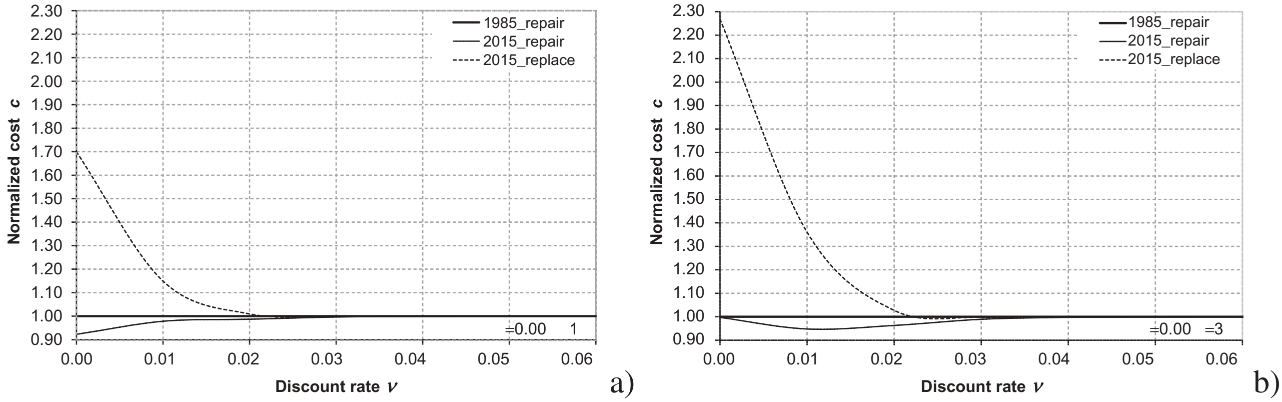

Figure 10. Effect of parameter χ on intervention costs (i.e., total repair total replacement). 2015 costs are normalized to 1985 repair costs. Figure 10a and 10b represent two different scenarios referred to relevance and duration of maintenance works.

$$C = C_T \frac{\nu(1+\nu)^T}{(1+\nu)^T - 1}. \tag{11}$$

Based on this cost model, different maintenance scenarios can be compared, and the optimal maintenance strategy related to the minimum life-cycle cost can be selected (Biondini, Frangopol, and Garavaglia 2008; Garavaglia and Sgambi 2016).

The weight χ in Equation (10) is the unit volume cost c_{kq} multiplier factor, which considers some matters usually involved in the maintenance process and affects the intervention costs. For example, if frequent but minor maintenance is limited to a small portion of the structure and requests a partial unavailability of the construction, the weight χ can be assumed as 1. Otherwise, if the maintenance involves the whole structure and total unavailability is needed for long, it significantly affects maintenance costs, and the weight χ can reach higher values.

6.2 Cost investigation applied to the case study

Equation (7) is applied for the estimation of the total cost related to the maintenance scenarios actualized by several discount rates ν.

In order to compare the three scenarios, the costs were normalized to the 1985 scenario (i.e., *1985 repair* = 1). Figure 10 a and b compare 2015 repair costs and the replacement costs. The fix cost $C_{\alpha q} = \alpha_q C_0$ was assumed equal to zero with $\alpha = 0$ for all the truss elements. After the disuse, the structure hasn't been subjected to service load anymore. Even if it has been affected by a significant environmental aggression since that time, a less-than-10% volume loss was registered in 2015 (compared to the value estimated in 1985). When the intervention cost (e.g., repair) in 2015 is compared with the same intervention but in 1985 (normalized at 1), considering a fluctuation in α-value, since the structure suffered a total volume loss of just 10% after 1985, it is clear that there would have been no significant cost-benefit if the same intervention was made in advance than 2015. Otherwise, a total replacement of the structure would have raised the cost considerably, at least up to a discount rate between 0.02 and 0.03.

Figure 10 a and b show the effect of the parameter χ on intervention costs. As said before, the weight χ is influenced by relevance and duration of maintenance works and it is clearly represented by comparing the total replacement scenario in Figure 10a with the one in Figure 10b.

Figure 11 compares the 2015 repair normalized to the 1985 repair related to each α-value (for the definition of parameter α refer to Section 5.1; it considers possible variations in fixed cost due to economic aspects related to different instants of time). A high value of α significantly affects the costs with discount ratio ν between 0.01 and 0.02. Furthermore, if the

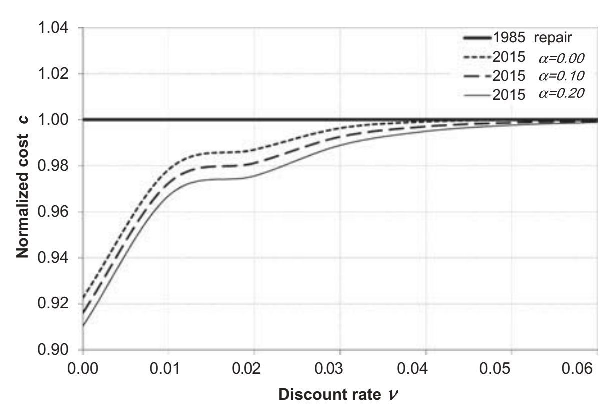

Figure 11. Effect of parameter α on 2015 repair costs normalized to 1985 repair costs.

PROOF ONLY

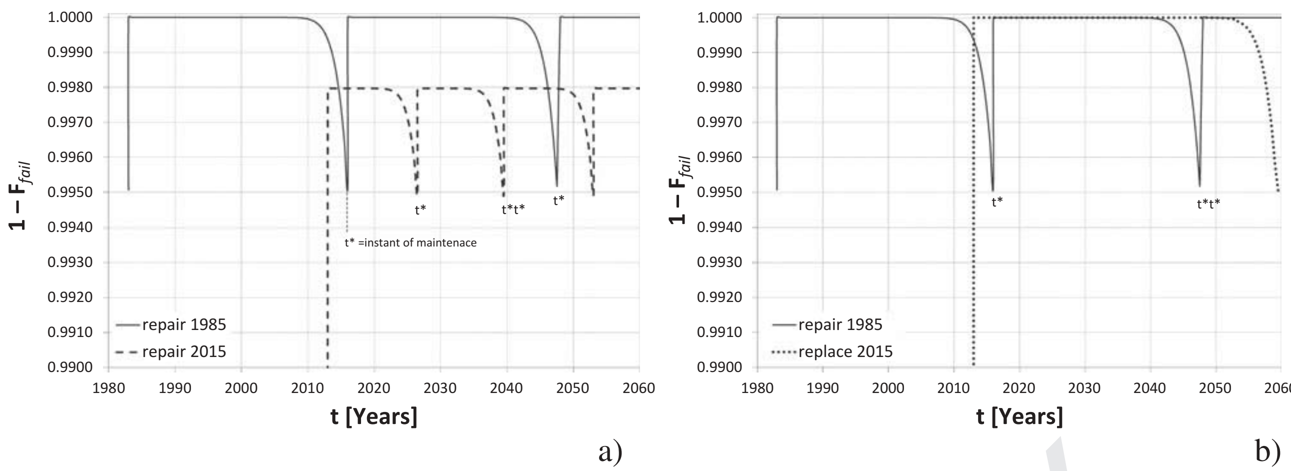

Figure 12. Maintenance scenarios: (a) 1985 total repair compared to 2015 total repair (performance 99.8%); and (b) 1985 total repair compared to 2015 total replacement. *t** refers to future instants of maintenance.

discount ratio exceed v = 0.04, the benefit of a late maintenance is nullified.

From the cost analysis it results that currently repairing is more convenient than replacing when the discount rate is lower than v = 0.03, while all scenarios are equivalent when v > 0.03.

6.3 Some remarks

The analysis here exposed suggests that total repair or local replacement interventions are the optimal solution for the specific case study. At present, the possible intervention scenarios are two: repair and restoration of the original volume, and replacement of the whole structure. The latter is the most invasive and not in accordance with the ideas of preservation and protection of historic constructions. Section 5.1 investigates the costs related to each scenario: repairing results more convenient than replacing the whole system. Furthermore, the 2015 repair appears to be less money-wasting than the 1985 repair.

It is important to remember that any intervention performed in the future must be supported by an adequate maintenance plan in order to preserve the structural integrity and identity. The method here described is useful for optimising the intervention schedule in terms of reliability, safety, and preservation of the historic heritage, and evaluating each scenario in terms of performance.

The three scenarios were analyzed as follows: repair in 1985 (83 years old), repair in 2015 (113 years old), full replacement in 2015. The deterioration process was modeled with the damage law in Figure 8; the threshold of acceptable risk was assumed as $(1 - F_{fail}) = 0.005$.

Figure 12 show and compares the scenarios: (a) repair in 1985 (100% performance recovered) and repair in 2015 (less-than-100% performance recovered); and (b) repair in 1985 and replacement in 2015.

If the structure had been repaired in 1985, it would have recovered the original performance level (i.e., undamaged state) and then it would have probably followed the deterioration pattern of the previous 80 years. In order to avoid the structural performance to exceed the threshold of acceptable risk equal to 0.005, this scenario should have required a cyclical maintenance each 30 years.

If the structure is repaired at present (115 years old) it will not fully recover the original performance level, and it will require a cyclical maintenance each 13–15 years (Figure 12a).

If the structure is replaced, the performance level is fully restored and the cyclical maintenance can be scheduled each 45–50 years (Figure 12b).

Hence, a simple cost-benefit analysis reveals that the high cost to replace the elements today results in long-term benefits with delayed maintenances; otherwise, the present benefit in repairing the damaged elements has to be compared with future maintenance costs and cultural value of the construction (whether it will be compromised or enhanced by the strategy adopted).

7. Conclusions

The research discusses a probabilistic approach to life-cycle assessment and rehabilitation strategy planning for existing deteriorating structures it terms of cost and performance (i.e., reliability, preservation, cost-benefit optimization, maintenance schedule, etc.).

PROOF ONLY

The method consists in a numerical code for structural analysis implemented with a damage law and a Monte Carlo simulation technique. This approach simulates a combined deterioration process (i.e., natural aging, usage, and weathering) affecting a system over time, in performance and structural response terms in order to define and evaluate efficient intervention scenarios for structural reliability and people safekeeping while preserving its historic and architectural integrity and identity.

The case study is a Polonceau truss of the old pig abattoir within the complex of the municipal slaughterhouse in Monza (close to Milan, Northern Italy). The construction was built in 1902, and abandoned in 1984.

In order to optimize the analysis model, the structural life was divided in two major phases: service life/pre-disuse (1902–1984; subjected to deterioration by natural aging and usage) and obsolescence/post-disuse (1985–present; subjected to degradation by negligence and weathering). These distinct periods have required the application of two different deterioration laws (Equation (3)).

The calibration of the two damage laws was executed using data collected during surveys in 1985, 2005, and 2015.

The Monte Carlo simulation pointed out that during the service life, aging and usage had reduced the volume of each structural element by 27%, while after the roofing collapsed in 1985 weathering and negligence had led to a 34–35% decrease in volume of almost the whole structural system.

The procedure has proven to be effective for the estimation of the probability of failure in the next interval Δt if it hasn't happened yet at instant t_0 (Equation (6)). In this regard, the probability of failure with $t_0 = 1985$ and $\Delta t = 1$ year, $P_{\Delta t=1|t_0=1984} = 0.0018$, and the probability with $t_0 = 2015$ and $\Delta t = 2$ years, $P_{\Delta t=2|t_0=2015}=0.128$, differ by two orders of magnitude. Considering these results, it is clear the urgency to intervene on this historic heritage.

The probabilistic simulation of volume loss suffered over time is the parameter for the development and cost-performance comparison of different rehabilitation strategies. When the actual possible scenarios are normalized to the repairs in 1985, a repair of damaged elements rather than replace the entire structure seems to be favorable in cost terms but not in performance terms. That is because repairs require a much more careful, tight maintenance plan, which might compromise the initial saving. In this regard, the historic value analysis of the construction holds the balance of power in deciding which of the scenarios is the most profitable, no matter the cost is. However, the approach here discussed results in decisions unquestionably aware of the relation between cost and risk in applying any scenario considered.

References

Avramidou, N. 1990. *Criteri di progettazione per il restauro delle strutture in cemento armato*. Liguori.

Bagnoli, P., M. Bonfanti, G. Della Vecchia, M. Lualdi, and L. Sgambi. 2015. A method to estimate concrete hydraulic conductivity of underground tunnel to assess lining degradation. *Tunnelling and Underground Space Technology* 50:415–23. doi:10.1016/j.tust.2015.08.008.

Baruchello, L., and G. Assenza. 2004. *Diagnosi dei dissesti e consolidamento delle costruzioni*, 3rd ed. DEI.

Bertolini, L., B. Elsener, P. Pedeferri, and R. P. Polder. 2004. *Corrosion of steel in concrete: Prevention, diagnosis, repair.* Weinheim: WILEY-VCH Verlag GmbH & Co. KGaA.

Binda, L. 1996. RILEM Committees, RILEM TC127-MS: Tests for masonry materials and structures. *Materials and Structures* 29 (192):459–75. ISSN: 1359-5997.

Binda, L., G. Baronio, E. D. Ferrieri, and P. Rocca, 1996a, Full-scale models for the calibration of laboratory aging test, Proceedings of 7DBMC, Stoccolm, Swiden, vol. II, 968–78.

Binda, L., G. Baronio, L. Gambarotta, S. Lagomarsino, and C. Modena, 1999, Masonry constructions in seismic areas of central Italy: A multi-level approach to conservation, Proceedings of 8NAMC North American Masonry Conf., Austin, TX, 44–55, CD-ROM.

Binda, L., G. Cardani, C. Gentile, L. Zanzi, and E. Massetti. 2009. Investigation, diagnosis and conservation design of the Church of St. Lorenzo in Cremona, Italy. In *Proceedings of Conf. Protection of Historical Buildings – PROHITECH 2009*, ed. F. M. Mazzolani, vol. I, 115–24, Roma, Italy. June 21–24, 2009, ISBN: 978-0-415-55803-7.

Binda, L., M. Lualdi, A. Saisi, and L. Zanzi. 2011. Radar investigation as a complementary tool for the diagnosis of historic masonry buildings. *International Journal of Materials and Structural Integrity* 5 (1):1–25. doi:10.1504/IJMSI.2011.039043.

Binda, L., C. Modena, M. R. Valluzzi, and R. Zago, 1996b, Mechanical effects of bed joint steel reinforcement in historic brick masonry structures, Proceeding of 8th Int. Conf. and Exhibition, Structural Faults + Repair, CD-ROM.

Binda, L., L. Zanzi, M. Lualdi, and P. Condoleo. 2005. The use of georadar to assess damage to a masonry Bell Tower in Cremona, Italy. *International Journal NDT&E* 38:171–79. doi:10.1016/j.ndteint.2004.03.010.

Biondini, F., F. Bontempi, and P. G. Malerba. 2004. Fuzzy reliability analysis of concrete structures. *Computers & Structures* 82 (13–14):1033–52. doi:10.1016/j.compstruc.2004.03.011.

Biondini, F., D. M. Frangopol, and E. Garavaglia. 2008. Life-cycle reliability analysis and selective maintenance of deteriorating structures. In *First International Symposium on Life-Cycle Civil Engineering (IALCCE'08), Varenna, Lake Como, Italy, June 10–14, 2008*, eds F. Biondini, and D. M. Frangopol, 483–88. London, UK: CRC Press, Taylor & Francis Group.

PROOF ONLY

Bontempi, F., L. Catallo, and L. Sgambi, 2004, Performance-based design and analysis of the Messina Strait Bridge, Second ASRANet International Colloquium, Barcelona, Spain, July 5–7.

Bruggi, M. 2014. Finite element analysis of no–Tension structures as a topology optimization problem. *Structural and Multidisciplinary Optimization* 50 (2014):957–73. doi:10.1007/s00158-014-1093-z.

Campanella, C. 2017. *Il rilievo degli edifici*. Dario Flaccovio Editore s.r.l.

Cardani, G., C. Tedeschi, L. Binda, and G. Baronio, 2001, Historic farms in Italy: Survey on effects of lack of maintenance, Proceedings of Int. Congr. More than Two Thousand Years in the History of Architecture Safeguarding the Structure of our Architectural Heritage, Bethlehem, Palestine, vol. 1, Section 1a, 1–6.

Ceravolo, R., A. De Stefano, and M. Pescatore. 2009. Change in dynamic parameters and safety assessment of civil structures. *Mechanics of Time-Dependent Materials* 12 (4):365–76. doi:10.1007/s11043-008-9063-8.

Ciampoli, M. 1998. Time dependent reliability of structural systems subject to deterioration. *Computers & Structures* 67 (1–3):29–35. doi:10.1016/S0045-7949(97)00153-3.

Ciampoli, M. 1999. A probabilistic methodology to assess the reliability of deteriorating structural members. *Computer Methods in Applied Mechanics and Engineering* 168 (1–4):207–20. doi:10.1016/S0045-7825(98)00141-8.

Cigni, G. 1978. *Il consolidamento murario, Tecniche d'intervento*. Edizioni Kappa.

Colombo, G. 1890. *Manuale dell'Ingegnere Civile e Industriale*, 11th ed. Hoepli.

Cruz, H., D. Yeomans, E. Tsakanika, N. Macchioni, A. Jorissen, M. Touza, M. Mannucci, and P. B. Lourenço. 2015. Guidelines for on-site assessment of historic timber structures. *International Journal of Architectural Heritage* 9 (3):277–89. doi:10.1080/15583058.2013.774070.

de Vent, I. A. E., S. Naldini, R. P. J. Van Hees, L. Binda, and A. Saisi. 2010. Definition of structural damage patterns: A structural damage atlas. *International Journal for Restoration of Buildings and Monuments* 16 (3):167–86. doi:10.1515/rbm-2010-6371.

Decò, A., and D. M. Frangopol. 2013. Life-cycle risk assessment of spatially distributed aging bridges under seismic and traffic hazards. *Earthquake Spectra* 29 (1):127–53. doi:10.1193/1.4000094.

Dell'Orto, C., L. M. Sanchez Jimenez, and M. Suma, 2015, *La città di Monza: Opportunità e valorizzazione delle aree dismesse. Il progetto di riuso per l'area dell'ex Macello Comunale*. MSc. Thesis., School of Civil Architecture, Politecnico di Milano.

Flanagan, R., G. M. J. Norman, and G. Robinson. 1989. *Life Cycle Costing – Theory and Practice*. Oxford, UK: BSP Professional Book.

Furuta, H., K. Ishibashi, K. Nakatsu, and S. Hotta. 2008. Optimal restoration scheduling of damaged networks under uncertain environment by using improved genetic algorithm. *Tsinghua Science and Technology* 13 (Suppl. 1):400–05. doi:10.1016/S1007-0214(08)70181-0.

Garavaglia, E., N. Basso, and L. Sgambi. 2012. The markovian approach for probabilistic life-cycle assessment of existing structures. *Applied Mathematics* 3 (12):2080–88. doi:10.4236/am.2012.312A287.

Garavaglia, E., A. Gianni, and C. Molina. 2004. Reliability of porous materials: Two stochastic approaches. *Journal of Materials in Civil Engineering* 16 (5):419–26. doi:10.1061/(ASCE)0899-1561(2004)16:5(419).

Garavaglia, E., and L. Sgambi. 2015. The use of a credibility index in the life-cycle assessment of structures. *Structure and Infrastructure Engineering* 11 (5):683–94. doi:10.1080/15732479.2014.896022.

Garavaglia, E., and L. Sgambi. 2016. Selective maintenance planning of steel truss bridge based on the Markovian approach. *Engineering Structures* 125 (2016):532–45. doi:10.1016/j.engstruct.2016.06.055.

Gregorczyk, P., and P. B. Lourenço. 2000. A review on flat-jack testing; *Engenharia civil, UM. Número* 9:39–50.

Hobbs, B., and M. Tchoketch Kebir. 2007. Non-destructive testing techniques for the forensic engineering investigation of reinforced concrete buildings. *Forensic Science International* 167 (2–3):167–72. doi:10.1016/j.forsciint.2006.06.065.

Koçak, A., and T. Köksal. 2010. An example for determining the cause of damage in historical buildings: Little hagia sophia (Church of St. Sergius and Bacchus) – Istanbul, Turkey. *Engineering Failure Analysis* 17 (4):926–37. doi:10.1016/j.engfailanal.2009.11.004.

Kong, J. S., and D. M. Frangopol. 2003. Life-cycle reliability-based maintenance cost optimization of deteriorating structures with emphasis on bridges. *Journal of Structural Engineering* 129 (6):818–24. doi:10.1061/(ASCE)0733-9445(2003)129:6(818).

Lagomarsino, S., and S. Cattari. 2015. PERPETUATE guidelines for seismic performance-based assessment of cultural heritage masonry structures. *Bulletin of Earthquake Engineering* 13 (1):13–47. doi:10.1007/s10518-014-9674-1.

Lo, T. Y., and K. T. W. Choi. 2004. Building defects diagnosis by infrared thermography. *Structural Survey* 22 (5):259–63. doi:10.1108/02630800410571571.

Lourenço, P. B. 2006. Recommendations for restoration of ancient buildings and the survival of a masonry chimney. *Construction and Building Materials* 20:239–51. doi:10.1016/j.conbuildmat.2005.08.026.

Lourenço, P. B., E. Luso, and M. G. Almeida. 2006. Defects and moisture problems in buildings from historical city centres: A case study in Portugal. *Building and Environment* 41:223–34. doi:10.1016/j.buildenv.2005.01.001.

Lourenço, P. B., and J. G. Rots. 1997. Multisurface interface model for analysis of masonry structures. *Journal of Engineering Mechanics* 123 (7):660–68. doi:10.1061/(ASCE)0733-9399(1997)123:7(660).

Lourenço, P. B., J. G. Rots, and J. Blaauwendraad. 1998. Continuum model for masonry: Parameter estimation and validation. *Journal of Structural Engineering* 124 (6):642–52. doi:10.1061/(ASCE)0733-9445(1998)124:6(642).

Lourenço, P. B., H. S. Sousa, R. D. Brites, and L. C. Neves. 2013. In situ measured cross section geometry of old timber structures and its influence on structural safety. *Materials and Structures* 46:1193–208. doi:10.1617/s11527-012-9964-5.

Mahin, S. A. 1998. Lessons from damage to steel buildings during the Northridge earthquake. *Engineering Structures* 20 (4–6):261–70. doi:10.1016/S0141-0296(97)00032-1.

The Mathworks, Inc. Software 2005. MatLab 7.1, Computer Code, http://www.mathworks.com.

PROOF ONLY

Melchers, R. E., and D. M. Frangopol. 2008. Probabilistic modeling of structural degradation. *Special Issue of Reliability Engineering & System Safety* 93 (3):363–500. doi:10.1016/j.ress.2007.01.001.

Milani, G., and P. B. Lourenço. 2010. Monte Carlo homogenyized limit analysis model for randomly assembled blocks in-plane loaded. *Computational Mechanics* 46 (6):827–49. doi:10.1007/s00466-010-0514-0.

Petrini, F., and F. Bontempi. 2011. Estimation of fatigue life for long span suspension bridge hangers under wind action and train transit. *Structure and Infrastructure Engineering* 7 (7–8):491–507. doi:10.1080/15732479.2010.493336.

Porro, A., and W. Vezzani, 2005, *Ex Macello a Monza: Rinascita di un'area strategica tra tradizione e trasformazione*. MSc. Thesis., IV School of Engineering, Politecnico di Milano.

Roca, P., M. Cervera, G. Gariup, and L. Pela'. 2010. Structural analysis of masonry historical constructions. Classical and advanced approaches. *Archives of Computational Methods in Engineering* 17 (3):299–325. doi:10.1007/s11831-010-9046-1.

Sandrinelli, G. 1905. *Resistenza dei Materiali e stabilità delle costruzioni ad uso degli ingegneri, capomastri e costruttori*. Hoepli. Q10

Schuller, M. P. 2003. Nondestructive testing and damage assessment of masonry structures. *Progress in Structural Engineering and Materials* 5 ((4),):239–51. doi:10.1002/pse.160.

Sousa, H. S., J. M. Branco, and P. B. Lourenço, 2014, Use of random sampling and Bayesian methods in the prediction of chestnut timber beams bending stiffness, Proceedings 2014 World Conference on Timber Engineering: Renaissance of Timber Construction, WCTE 2014, Quebec City, Canada; August 10, 2014 through August 14, 2014, Code 110957.

Yang, J. N., Y. Lei, S. Lin, and N. Huang. 2004. Hilbert-huang based approach for structural damage detection. *Journal of Engineering Mechanics* 130 (1). doi:10.1061/(ASCE)0733-9399(2004)130:1(85).

Yoa, G. C., K. C. Chang, and G. C. Lee. 1992. Damage diagnosis of steel frames using vibration signature analysis. *Journal of Engineering Mechanics* 118 (9):1949–61. doi:10.1061/(ASCE)0733-9399(1992)118:9(1949)-9399(1992)118:9(1949).

PROOF ONLY